

Decoherence and collective effects of quantum emitters near a medium at criticality

F. M. D'Angelis, F. A. Pinheiro, and F. Impens

Instituto de Física, Universidade Federal do Rio de Janeiro, Caixa Postal 68528, Rio de Janeiro 21941-972, RJ, Brazil

(Received 25 March 2019; revised manuscript received 9 May 2019; published 28 May 2019)

We investigate the influence of phase transitions on the behavior of collective quantum emission. We discuss two distinct physical processes, the center-of-mass decoherence of a single emitter, and the collective emission of two emitters, addressed with a unified formalism relying on standard perturbation theory. Two specific examples of phase transitions are considered: the percolation transition in a metal-dielectric composite, and the metal-insulator transition in VO₂. The decoherence and the collective emission rates can be decomposed as a sum of two contributions, accounting for the spontaneous emission and for interference effects, respectively. The former is enhanced by the Purcell effect for emitter(s) in the vicinity of the critical medium. The latter, associated with quantum interferences, experiences a “sudden death” near the critical point of the phase transition. Our findings unveil the interplay between the Purcell and collective effects and its dependence on metal-insulator transitions. In the case of VO₂, decoherence and collective emission rates exhibit a characteristic hysteresis that strongly depends on the material temperature. These results, based on experimental data, suggest that VO₂ could be explored as a versatile material platform where decoherence and collective emission can be tuned by varying the temperature.

DOI: [10.1103/PhysRevB.99.195451](https://doi.org/10.1103/PhysRevB.99.195451)**I. INTRODUCTION**

The study of collective effects has a long history in the context of spontaneous emission from an ensemble of quantum emitters (atoms, molecules, or quantum dots) in both optical cavities and free space. The pioneering work of Dicke [1] has shown that the intensity radiated by N atoms placed at subwavelength distances may scale as N^2 for specific global quantum states of the emitters. This phenomenon, known as superradiance, arises from constructive interferences in the collective emission process. More recently, progress in the field of nanophotonics has motivated and enabled the experimental investigation of superradiance in a broad range of photonic environments. Relevant examples are the coupling of quantum emitters (atoms, molecules, and quantum dots) to plasmonic waveguides [2], microcavities [3,4], metallic interfaces [5], and epsilon-near-zero metamaterials [6]. Tailoring and tuning collective optical effects enables one to enhance on-demand light-matter interactions at the nanoscale. In order to develop novel photonic applications where the collective spontaneous emission rate of several quantum emitters can be tuned, material platforms such as plasmonic waveguides [7], graphene-based structures [8], and nanofibers [9] have been considered. In this line, collective effects, combined with a suitable photonic environment, also have interesting applications in the field of quantum control. Collective effects can be used to put two ions in a maximally entangled state near a cavity [10] or to obtain a tunable two-qubit entanglement in a graphene waveguide [11]. Previous work has considered using subradiance [12–16]—the counterpart of superradiance associated with an inhibition of radiation through destructive interferences—for quantum memories [17], nanolasers [18], and quantum computers [19].

On the other hand, a key element to achieve reliable quantum control is the design of a quantum environment minimizing decoherence [20]. The design of such an environ-

ment is a prerequisite when considering quantum information processing architectures at the nanoscale, where fluctuation-induced phenomena may predominate and compete with coherent processes. In this line, it has been shown that Casimir-Polder forces may be strongly affected by collective effects [21], resulting from an interplay between the Purcell [22] and the Dicke effects [23]. This approach suggests that collective effects and fluctuation-induced phenomena should be apprehended together.

In this paper, we put forward a strategy that combines an alternative material platform, composite media and vanadium dioxide (VO₂), and a specific physical mechanism, critical phenomena, to achieve control of either collective effects of several emitters or center-of-mass (c.m.) decoherence of a single emitter. There is evidence, both theoretical [24–26] and experimental [27], that phase transitions affect the spontaneous emission of a single emitter in a crucial way. This has been recently confirmed theoretically, setting the grounds for the determination of critical exponents via the Purcell factor [28]. However, the effect of phase transitions in the collective emission or in the c.m. decoherence of quantum emitters remains to be explored. Controlling this decoherence rate is particularly relevant in quantum architectures using the c.m. to store and process quantum information [29].

Here, we fill this gap by investigating the collective emission of two-level quantum emitters and the c.m. decoherence of a single emitter near a composite medium that undergoes a percolation phase transition. We use a formalism developed in the context of surface-induced dynamical Casimir phases [30–32], which enables an analogy between collective effects and the decoherence rate of a delocalized emitter [33]. We obtain a description of the c.m. decoherence rate as a function of the order parameter of the material phase transition. In particular, we demonstrate the strong suppression of the interference contribution to both the decoherence and to the collective

emission rates in the presence of a media undergoing a percolation phase transition. We also investigate the specific example of the metal-insulator transition in a VO₂ material, to show that the decoherence and collective emission rates can exhibit a characteristic temperature-dependent hysteresis. Altogether, our findings not only unveil the role of critical phenomena on collective emission and c.m. decoherence, but they also suggest that VO₂ could be explored as an alternative material platform to control these processes via thermal effects.

II. METHODOLOGY

In this section, we describe the theoretical tools that will be used to address simultaneously two distinct physical phenomena in the vicinity of a medium undergoing a phase transition: the decoherence of a single emitter in a quantum superposition of two wave packets, and the spontaneous emission of two quantum emitters. In the following, we show that these two distinct physical phenomena can be described by the same theoretical framework, which enables us to unveil the role of interference effects in both situations.

A. Interaction of the emitter with the light field

The interaction of the emitter with the light field is described by a dipolar Hamiltonian $H(\mathbf{r}, t) = -\mathbf{d}(t) \cdot \mathbf{E}(\mathbf{r}, t)$, involving the dipole operator $\mathbf{d}(t)$ and the quantized electric field operator $\mathbf{E}(\mathbf{r}, t)$ taken at the position \mathbf{r} of the quantum emitter [34]. We work from now on in the interaction picture, letting the dipole and light field operators evolve according to the free dipolar and light field Hamiltonians. To obtain quantitative estimates of the decoherence rates, we have taken this emitter as a two-level atom with a transition wavelength $\lambda_0 = 450 \mu\text{m}$.

B. Electric field Green's function

The Green's dyadic in the vicinity of a bulk material contains a free part and a scattered part [35],

$$G(\mathbf{r}_1, \mathbf{r}_2; \omega_0) = G^0(\mathbf{r}_1, \mathbf{r}_2; \omega_0) + G^{\text{Sca}}(\mathbf{r}_1, \mathbf{r}_2; \omega_0), \quad (1)$$

where $G^0(\mathbf{r}_1, \mathbf{r}_2; \omega_0)$ and $G^{\text{Sca}}(\mathbf{r}_1, \mathbf{r}_2; \omega_0)$ are the free and scattering Green's dyadic, respectively. We shall consider situations where the two wave packets (or two quantum emitters) are located at the same height z with respect to the material surface, and at a distance x as depicted in Fig. 1. We shall also use the free and scattering contributions to the Green's function trace, denoted by $\mathcal{G}^0(\mathbf{r}_1, \mathbf{r}_2; \omega_0)$ and $\mathcal{G}^{\text{Sca}}(\mathbf{r}_1, \mathbf{r}_2; \omega_0)$, respectively,

$$\begin{aligned} \mathcal{G}^0(\mathbf{r}_1, \mathbf{r}_2; \omega_0) &= \frac{i}{2\pi} \int_0^\infty \frac{k_\parallel}{k_z} J_0(k_\parallel x) dk_\parallel, \quad (2) \\ \mathcal{G}^{\text{Sca}}(\mathbf{r}_1, \mathbf{r}_2; \omega_0) &= \frac{i}{4\pi} \int_0^\infty \frac{k_\parallel}{k_z} J_0(k_\parallel x) \left[r^{\text{TE,TE}} \right. \\ &\quad \left. + \frac{c^2}{\omega_0^2} r^{\text{TM,TM}} (k_\parallel^2 - k_z^2) \right] e^{2ik_z z} dk_\parallel. \quad (3) \end{aligned}$$

ω_0 is the transition frequency, J_0 is the zero-order spherical Bessel function, and $r^{\text{TE,TE}}$ ($r^{\text{TM,TM}}$) is the Fresnel reflection coefficient for transverse electric (TE) [transverse magnetic (TM)] polarization. The integration in the region $k_\parallel < \omega_0/c$ corresponds to the contribution of progressive waves with

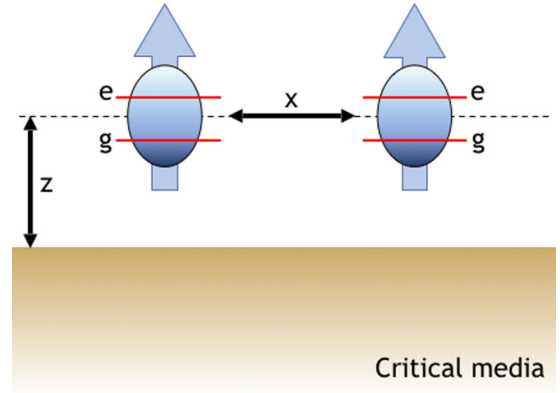


FIG. 1. Schematic view of the systems under consideration, showing a representation of the two atoms or wave packets for a two-level quantum emitter, separated by a distance x from each other and at a distance z to the material. In the case of two emitters we consider both to be with the dipoles aligned in the z direction, while for the single emitter in a superposition of wave packets we average over orientations.

$k_z = \sqrt{k_0^2 - k_\parallel^2}$. In the scattering wave function, the integration in the range $k_\parallel > \omega_0/c$ induces a contribution of evanescent waves with $k_z = i\sqrt{k_\parallel^2 - k_0^2}$, which play an important role in the collective emission and c.m. decoherence.

C. Modeling the optical properties of the materials

We model the optical properties of the semi-infinite, non-magnetic critical media via the Bruggeman effective medium theory (BEMT) [36,37], which is one of the simplest analytical models that can predict the percolation phase transition. This model is well suited for the two phase transitions considered below, namely, the percolation transition in a metal-dielectric composite material and the metal-insulator transition in VO₂ [38]. The system considered for the percolation transition is a polystyrene host medium filled with gold inclusions. In the VO₂ material, metallic clusters are formed as the temperature increases, so that they can also be treated as effective metallic inclusions. VO₂ is particularly interesting for photonic and electronic applications because its transition occurs near room temperature, allowing for novel applications such as metamaterial reflectors and switches [39,40]. This enables one to address both phase transitions with the same effective model theory, where the relevant critical parameter is the filling factor f representing the fraction of the volume occupied by these inclusions. The effective permittivity ϵ_{eff} is the solution with a positive imaginary part (as expected for a passive medium) of the following equation [36,37],

$$\begin{aligned} (1-f) \left(\frac{\epsilon_{\text{hm}} - \epsilon_{\text{eff}}}{\epsilon_{\text{eff}} + L(\epsilon_{\text{hm}} - \epsilon_{\text{eff}})} + \frac{4(\epsilon_{\text{hm}} - \epsilon_{\text{eff}})}{2\epsilon_{\text{eff}} + (1-L)(\epsilon_{\text{hm}} - \epsilon_{\text{eff}})} \right) \\ + f \left(\frac{\epsilon_i - \epsilon_{\text{eff}}}{\epsilon_{\text{eff}} + L(\epsilon_i - \epsilon_{\text{eff}})} + \frac{4(\epsilon_i - \epsilon_{\text{eff}})}{2\epsilon_{\text{eff}} + (1-L)(\epsilon_i - c)} \right) = 0, \quad (4) \end{aligned}$$

where ϵ_{hm} and ϵ_i are the host medium and inclusion permittivities, respectively, and L is the depolarization factor

related to the geometry of the inclusions. In the percolation transition, the filling factor f and the geometry of the inclusions can be chosen independently from the temperature. Here, we consider spherical inclusions corresponding to a depolarization factor $L = 1/3$. Differently, for VO_2 , the depolarization factor L , the filling fraction f , and the insulator (metallic) permittivities ϵ_{hm} (ϵ_i) are determined by the temperature T . In the latter, we have used a relation between the filling fraction f and the depolarization factor L based on the experimental data reported in Ref. [41]. For both materials, the phase transition occurs at the critical value of the filling factor $f = 1/3$, for which the effective permittivity ϵ_{eff} becomes purely imaginary [36,37].

1. Metal-dielectric composite undergoing a percolation transition

In order to describe the material parameters, we use the Drude model for the inclusions and the Drude-Lorentz model for the host medium, with parameters extracted from experiments. According to these models, the permittivity is expressed as $\epsilon_i(\omega) = 1 - \omega_{p_i}^2/(\omega^2 + i\gamma_i\omega)$ for the gold inclusions and as $\epsilon_{\text{hm}}(\omega) = 1 + \sum_j \omega_{p_j}^{\text{hm}2}/(\omega_{R_j}^2 - \omega^2 - i\Gamma_j\omega)$ for the host medium. We have introduced the plasma frequencies for the inclusions ω_{p_i} and the oscillating strengths $\omega_{p_j}^{\text{hm}}$ for the host medium, as well as the inverse of the relaxation times γ_i and Γ_j for the inclusions and for the host medium, respectively, and the resonant frequencies ω_{R_j} . The experimental values of these parameters were extracted from Refs. [42,43].

2. VO_2 material undergoing a metal-insulator phase transition

In contrast to the metal-dielectric composite, the permittivities of the VO_2 material now rely completely on real experimental data taken from a thin film of 200 nm thickness and deposited over a 1-mm-thick sapphire (Al_2O_3) substrate [41]. As a manifestation of the material hysteresis, there is a discrepancy in the temperatures associated with the phase transition in the cooling and heating cycles. Indeed, the phase transition occurs at the temperature $T \approx 342$ K for the heating cycle and at the temperature $T \approx 336$ K for the cooling cycle [41].

III. CENTER-OF-MASS DECOHERENCE OF A SINGLE EMITTER NEAR A CRITICAL MEDIUM

In this section, we investigate the decoherence rate suffered by a delocalized single quantum emitter near a material undergoing a phase transition. Specifically, we consider a neutral two-level atom with no permanent dipole, but most of the discussion could be extended to other quantum emitters. The decoherence rate involves two contributions [33], corresponding to a first term simply associated with the global photon emission rate, and a second term involving quantum interferences and related to the quality of the which-way information. We study the interplay between these two contributions as the material undergoes a phase transition. As demonstrated below, near the critical point of the transition, the contribution associated with interference effects is drastically suppressed.

A. Problem statement and general discussion

As in Ref. [33], we assume that a single quantum emitter is initially in an excited state, and that its c.m. wave function involves a superposition of two well-separated wave packets with negligible overlap. We monitor here the external degrees of freedom (DOF) of this quantum emitter (the considered quantum system), which may produce at most a single photon. The DOF of the emitter, the light field, and the material DOF play the role of an environment surrounding the quantum system. The phase transition affects the conductivity properties of the material and thus influences this environment. By virtue of the Purcell effect [22], the presence of the material near the emitter significantly increases the photonic emission. This phenomenon has been shown to be greatly enhanced near the critical point of the phase transition [26]. As the emitted photon may reveal the position of the emitting wave packet, the decoherence rate suffered by the wave function of the quantum emitter is also drastically increased near the critical point.

The discussion to follow focuses, however, on a more subtle influence on decoherence. Beyond the rate of photonic emission, the decoherence rate also depends on the quality of the which-way information contained in the emitted photon. The amount of which-way information depends in turn on the intrinsic features of light propagation, as well as on the distance between the wave packets composing the quantum emitter wave function. For instance, the emission of a long-wavelength (larger than the wave-packet separation) photon would hardly affect the wave function of the emitter, as an observer could not reliably infer from a field measurement the emitting wave packet. In contrast, the emission of a short-wavelength photon is expected to destroy the wave-function coherence, as an observer could in principle identify unambiguously the emitting wave packet. As the production of a long-wavelength photon carries poor-quality which-way information, it is associated with a negative interference contribution to the decoherence rate (“recoherence” rate) which almost cancels the contribution proportional to the photonic emission [33].

More generally, the structure of the electric field Green’s function affects the amount of which-way information per emitted photon. In the following, we discuss the importance of the scattering contribution to the Green’s function. Indeed, as the material undergoes a phase transition, the scattering contribution to the electric field Green’s function exhibits a sharp variation, which strongly reduces proportionally the interference contribution to the decoherence rate.

B. General expressions of the local and nonlocal decoherence rates

For convenience, we first recall the definition of the non-local and local decoherence rates [33]. We take the initial quantum state of the two-level atom as a product state $|\Psi(0)\rangle = |e\rangle \otimes \frac{1}{\sqrt{2}}(|\psi_+\rangle + e^{i\theta_0}|\psi_-\rangle)$, and assume the light field to be initially in the vacuum state. $|\psi_{\pm}\rangle$ denote external wave packets of a size assumed to be much smaller than the transition wavelength. The local and nonlocal decoherence rates can be obtained by considering the corresponding

imaginary phases in the long-time limit [33],

$$\Gamma_{L,NL}^{\text{Dec}} = \lim_{\Delta t \rightarrow \infty} \frac{1}{\Delta t} \text{Im}[\varphi_{L,NL}(\Delta t)]. \quad (5)$$

The complex local $\varphi_L(\Delta t)$ and nonlocal $\varphi_{NL}(\Delta t)$ phases arise from the dipolar interaction during the duration Δt , and are given by standard time-dependent perturbation theory as

$$\begin{aligned} \varphi_L(\Delta t) &= \frac{i}{2\hbar^2} \sum_{k=1,2} \int_0^{\Delta t} d\tau \int_0^{\Delta t} d\tau' \langle H(\mathbf{r}_k, \tau) H(\mathbf{r}_k, \tau') \rangle, \\ \varphi_{NL}(\Delta t) &= -\frac{i}{\hbar^2} \int_0^{\Delta t} d\tau \int_0^{\Delta t} d\tau' \langle H(\mathbf{r}_1, \tau) H(\mathbf{r}_2, \tau') \rangle. \end{aligned} \quad (6)$$

The local phase contains a sum of two contributions involving a single wave packet, while the nonlocal phase cannot be split in such separate single-wave-packet terms. The local decoherence rate is always positive, while the nonlocal decoherence can be of either sign, and is always negative when the wave packets become sufficiently close.

The total decoherence rate is given by the sum of these two contributions $\Gamma^{\text{Dec}} = \Gamma_L^{\text{Dec}} + \Gamma_{NL}^{\text{Dec}}$. To make the formal analogy with the superradiant emission more transparent, we shall consider the ratio of the total decoherence rate to the local decoherence rate $\Gamma^{\text{Dec}}/\Gamma_L^{\text{Dec}} = 1 + \Gamma_{NL}^{\text{Dec}}/\Gamma_L^{\text{Dec}}$. Indeed, when the wave-packet distance is larger than several transition wavelengths, the quantum interference contribution to the decoherence rate becomes negligible ($\Gamma_{NL}^{\text{Dec}} \ll \Gamma_L^{\text{Dec}}$) and thus the decoherence rate coincides with the spontaneous emission rate. This situation is in formal analogy to the incoherent spontaneous emission of sufficiently distant atoms. In the opposite limit, when the two wave packets are close enough, the interference contribution may reduce and eventually cancel the total decoherence rate, which is analogous to the Dicke superradiance of two emitters at subwavelength distance. The main difference is the presence of a minus sign in the nonlocal decoherence rate. A diminution of the c.m. decoherence of a single emitter is thus formally equivalent to an enhancement of the collective photonic emission.

The local and nonlocal phases (6) involve second-order correlation functions between the dipole and the electric field operators at different times and positions. The dipole correlations are expressed as $\langle e|d_i(0)d_j(\tau)|e \rangle = \frac{1}{3}\delta_{ij}|\mathbf{d}|^2 e^{i\omega_0\tau}$, with ω_0 the transition frequency. The local and nonlocal decoherence rates can then be recast in terms of the trace of the Green's dyadic $\mathcal{G}(\mathbf{r}, \mathbf{r}'; \omega_0) = \text{Tr} G(\mathbf{r}, \mathbf{r}'; \omega_0)$ [35],

$$\Gamma_L^{\text{Dec}} = \frac{\pi c}{\omega_0} \Gamma_0 \text{Im} \mathcal{G}(\mathbf{r}_1, \mathbf{r}_1; \omega_0) + \mathcal{G}(\mathbf{r}_2, \mathbf{r}_2; \omega_0), \quad (7)$$

$$\Gamma_{NL}^{\text{Dec}} = -\frac{2\pi c}{\omega_0} \Gamma_0 \text{Im} \mathcal{G}(\mathbf{r}_1, \mathbf{r}_2; \omega_0), \quad (8)$$

where $\Gamma_0 = \omega_0^3 |\mathbf{d}|^2 / (3\pi \hbar \epsilon_0 c^3)$ is the spontaneous emission rate. As a consistency check, in the absence of a scattering contribution to the Green's function [i.e., $\mathcal{G}(\mathbf{r}, \mathbf{r}'; \omega_0) = \mathcal{G}^0(\mathbf{r}, \mathbf{r}'; \omega_0)$], by using Eqs. (2), (7), and (8), one retrieves the free-space decoherence rate [33].

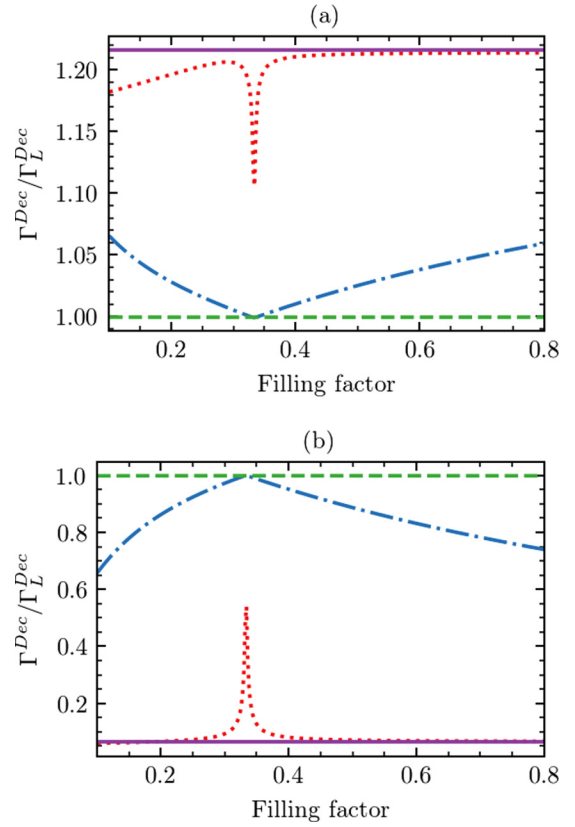


FIG. 2. Normalized decoherence rates $\Gamma^{\text{Dec}}/\Gamma_L^{\text{Dec}}$ for a superposition of two wave packets separated by a distance (a) $x = 0.7\lambda_0$ and (b) $x = 0.1\lambda_0$ as a function of the filling factor f and for different distances z to the composite metal-dielectric material. Here, we consider $z = 10^{-2}\lambda_0$ (red dotted line), $z = 10^{-3}\lambda_0$ (blue dash-dotted line), and $z = 10^{-4}\lambda_0$ (green dashed line). The values of the decoherence rates with no material are also plotted (solid purple lines). Decoherence rates have been obtained from Eqs. (7) and (8) by considering $\lambda_0 = 450 \mu\text{m}$ and the material properties described in Sec. II C.

C. Decoherence near a material undergoing a percolation transition

We have studied the ratio of the decoherence rates $\Gamma^{\text{Dec}}/\Gamma_L^{\text{Dec}}$ for two specific configurations corresponding to different distances between the wave packets. The results are shown in Fig. 2. In the first configuration, the separation between the two wave packets corresponds to $x = 0.7\lambda_0$. For this separation, the decoherence rate in the vacuum is increased by interference effects, and is roughly 20% larger than the spontaneous emission rate. In this case, each emitted photon carries which-way information enhanced by interference effects (i.e., greater than that at infinite wave-packet separation). In the second configuration, we consider a wave-packet separation of $x = 0.1\lambda_0$ yielding a free-space decoherence rate reduced to only 7% of the spontaneous emission rate, and thus associated with which-way information per photon of low quality. For each wave-packet separation, we have considered various distances from the material and the filling factor f across the critical region. The results, presented in Fig. 2, show that for distances extremely close to the plate $z \simeq 10^{-4}\lambda_0$, the nonlocal decoherence rate is suppressed for any value of the

filling factor f . For values of the distances z to the material such that $10^{-2}\lambda_0 \leq z \leq 10^{-3}\lambda_0$, one observes a striking change in the competition between the local and nonlocal decoherence contributions to the decoherence rate. When the filling factor f parameter is far from the critical region $f \simeq 1/3$, the total decoherence rate is close to its free-space value, resulting from the interplay between the nonlocal and the local decoherence rates. Close to the critical value $f_0 = 1/3$, however, the total decoherence rate tends towards the local decoherence rate. This shows that interference effects are strongly suppressed in the vicinity of the region $f \simeq f_0$ corresponding to the phase transition. In both configurations [Figs. 2(a) and 2(b)], the total decoherence rate tends towards the spontaneous emission rate, regardless of the quality of information contained in each photon. The decoherence rate, considered as a function of the filling factor f , presents a slope discontinuity as the filling factor f reaches the critical value $f_0 = 1/3$, suggesting that the percolation transition leads to a “sudden death” of the interference contribution to the decoherence rate. Indeed, the phase transition induces an abrupt change in the interplay between the decay channels contributing to the decoherence rate. Finally, one sees that the material exerts a significant influence on the total decoherence rate over a larger range of distances as the filling factor approaches its critical value.

One notes, in Fig. 2(a), an asymmetric profile of the decoherence rate as a function of the filling factor f at the wave-packet separation $x = 0.7\lambda_0$. For $f \geq 0.4$, the composite material is in the metallic phase and the c.m. decoherence rate remains close to the free-space value independently of the exact value of f . Differently, in the insulator phase ($f < 0.3$), the c.m. decoherence rate falls below its free-space value. This may be due to the fact that, in the metallic phase, the scattering c.m. decoherence contribution exhibits similar interferences as the free-space contribution [44].

Our findings show that the material exerts an influence on the c.m. decoherence on a range of distances z such that $z < z_0 \simeq 10^{-2}\lambda_0$. The discussion done in Ref. [26] suggests an interpretation in terms of evanescent waves. Due to their exponential attenuation by a factor $\exp(-4\pi z/\lambda_0)$, evanescent waves contribute only for emitters in the vicinity of the material. In Ref. [26], it was shown that the Purcell effect becomes material dependent for distances $z < 10^{-2}\lambda_0$ where the nonradiative decay is significant, which coincides with our observation on the c.m. decoherence rate.

D. Decoherence near a VO₂ material undergoing a metal-insulator transition

We investigate here the decoherence rate near VO₂. Figure 3(a) reveals that the phase transition suppresses the coherent contribution so that $\Gamma^{\text{Dec}}/\Gamma_L^{\text{Dec}} \rightarrow 1$. Figure 3(b) sketches the normalized decoherence rate in the phase transition during the heating cycle. This figure suggests that, when the material undergoes a phase transition, it may suppress the interference contribution to decoherence over a larger range of distances z between the material and the two wave packets. Further away from the material, the hysteresis is strongly reduced and the decoherence rate becomes almost insensitive to the material properties. On the other hand, for small dis-

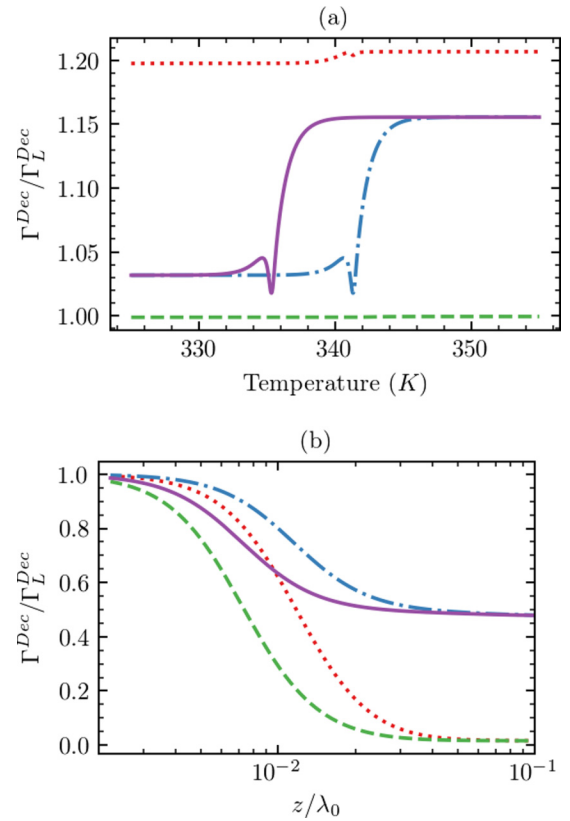


FIG. 3. Normalized decoherence rates $\Gamma^{\text{Dec}}/\Gamma_L^{\text{Dec}}$ in the vicinity of VO₂ undergoing a phase transition. (a) Decoherence rate as a function of temperature T for different distances z to the material with a fixed separation $x = 0.7\lambda_0$ between the wave packets. At the distance $z = 10^{-2}\lambda_0$, one notes a hysteresis leading to different values for the cooling cycle (solid purple line) and the heating cycle (blue dashed-dotted line). At the distance $z = 10^{-3}\lambda_0$ (green dashed line) (red dotted line), the cooling and heating curves become indistinguishable with the chosen scale. At the larger distance $z = 10^{-1}\lambda_0$, the hysteresis is very small (we have presented the cooling curve). (b) Decoherence rate as a function of the distance z to the material for different wave-packet separations at a fixed temperature $T = 342$ K. We have used $x = 0.05\lambda_0$ and $x = 0.3\lambda_0$ for both the heating cycle (red dotted and blue dashed-dotted lines, respectively) and the cooling cycle (green dashed and purple solid lines, respectively). We have taken $\lambda_0 = 450$ μm .

tances z to the material, the lines for the heating and cooling cycles merge, and the normalized decoherence rate become independent of the wave-packet separation [Fig. 3(b)]. This suggests that in the immediate vicinity of the material the decoherence rate is mostly determined by the contribution associated with the Purcell-enhanced spontaneous emission.

IV. COLLECTIVE DECAY NEAR CRITICAL MEDIA

A. Collective decay with prescribed dipoles

We first recall the collective decay rate Γ for a pair of quantum emitters, with prescribed dipole moments $\mathbf{d}_k = d_k \mathbf{u}_k$ oscillating in phase along fixed directions \mathbf{u}_k in the vicinity of a semi-infinite material. This semiclassical approach is well suited to describe superradiance from a collective symmetric

quantum state of the two emitters. The global emission rate can be expressed in terms of the electric field Green's dyadic (1) $G(\mathbf{r}, \mathbf{r}; \omega_0)$ evaluated at the emitter positions $\mathbf{r}_{m,n}$ [8],

$$\Gamma = \sum_{m=1,2} \sum_{n=1,2} \Gamma_{mn},$$

$$\Gamma_{mn} = \frac{2\omega_0^2}{\hbar\epsilon_0 c^2} \text{Im}[\mathbf{d}_n G(\mathbf{r}_n, \mathbf{r}_m, \omega_0) \mathbf{d}_m]. \quad (9)$$

This decay rate can be written as the sum of an incoherent contribution $\Gamma_I = \Gamma_{11} + \Gamma_{22}$ associated with the decay of two independent emitters near the surface and a coherent contribution $\Gamma_C = \Gamma_{12} + \Gamma_{21}$ encoding interference effects in the emission process [8]. Note that the coherent term Γ_C corresponds to the additional collective emission due to the simultaneous presence of several emitters. One may identify two distinct regimes, namely, the regime of superradiance for which $\Gamma_C > 0$ with an enhanced collective emission, and the regime of subradiance for which $\Gamma_C < 0$ with an inhibited collective emission. The incoherent contribution describes the usual Purcell effect experienced by a single emitter [26], and can be derived from the Fresnel coefficients of the material as

$$\frac{\Gamma_I}{\Gamma_0} = \frac{3c^3}{2\omega_0^3} \text{Re} \left[\int_0^\infty dk_{\parallel} \frac{k_{\parallel}^3}{k_z} (1 + r^{\text{TM, TM}} e^{2ik_z z}) \right]. \quad (10)$$

On the other hand, the coherent contribution Γ_C captures the interplay between the collective effects and the Purcell effect, which may drastically change as the material undergoes a phase transition. The coherent contribution reads

$$\frac{\Gamma_C}{\Gamma_0} = \frac{3c^3}{2\omega_0^3} \text{Re} \left[\int_0^\infty dk_{\parallel} \frac{k_{\parallel}^3}{k_z} J_0(k_{\parallel} x) (1 + r^{\text{TM, TM}} e^{2ik_z z}) \right]. \quad (11)$$

We focus on this last term in order to unveil the influence of phase transitions on collective quantum emission. We investigate two different physical situations, namely, the percolation metal-insulator transition in inhomogeneous media and the specific case of VO₂, where the phase transition is driven by the temperature.

B. Collective decay at the percolation transition

We now discuss the role of the percolation phase transition in the collective decay of two quantum emitters. We consider a specific geometry where both emitters are equidistant from the material and with parallel dipole orientations—orthogonal to the medium interface taken as a plane.

Figure 4 presents the normalized global decay rate Γ/Γ_I as a function of the filling fraction f of gold inclusions in a polystyrene host for different values of the emitter-material distance z between the emitters and the semi-infinite inhomogeneous medium. It reveals that at distances much smaller than the transition wavelength, typically of the order $z/\lambda_0 \simeq 10^{-4}$, crosstalks between the two quantum emitters are totally suppressed so that the incoherent contribution Γ_I predominates for all f . On the other hand, for larger distances of typically $z \gtrsim 0.1\lambda_0$, the material properties of the compound hardly affect the emission. For these distances, the material-dependent nonradiative contributions to the collective emission are strongly attenuated. In this limit the emission

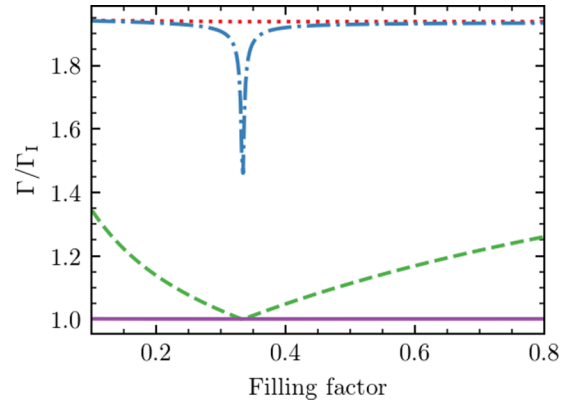


FIG. 4. Normalized spontaneous emission rate in the composite material for the symmetric state as a function of the filling factor f at a separation $x = 0.1\lambda_0$ between emitters with transition wavelength $\lambda_0 = 450 \mu\text{m}$. The normalized emission rate was calculated by considering Eqs. (10) and (11) and the effective permittivity described in Sec. II C. The dotted red, blue dashed-dotted, green dashed, and purple solid lines correspond to distances $z = 10^{-1}\lambda_0$, $z = 10^{-2}\lambda_0$, $z = 10^{-3}\lambda_0$, and $z = 10^{-4}\lambda_0$ from the material, respectively.

process is entirely governed by crosstalks between the emitters. For this range of distances, one has $\Gamma \approx 2\Gamma_I$ for all f , which correspond to a maximal superradiance. Remarkably, at the critical point $f = 1/3$ and for an intermediate range of emitter-material distances, there is a strong reduction of the coherent contribution to the total emission rate. In other words, collective effects are strongly suppressed at the critical point. As the collective contribution disappears with a slope discontinuity at the percolation threshold, one may speak of a “sudden death” of collective effects at the critical point—as shown previously for the interference contribution to the total decoherence rate.

C. Collective emission in the vicinity of a metal-insulator VO₂ transition

We now investigate the collective emission effects in the vicinity of a VO₂ material undergoing a metal-insulator phase transition. We consider again the previous geometry, with two quantum emitters at a fixed subwavelength separation $x = 0.1\lambda_0$ and at the same distance z from the interface. Figure 5 shows the collective emission for different values of this distance z . Figure 5, where the normalized global decay rate Γ/Γ_I is calculated as a function of the temperature T , demonstrates that the characteristic hysteresis of VO₂ also shows up on collective quantum emission. Interestingly, this implies that the total decay rate of the system will not only strongly depend on the temperature but also on whether one is cooling or heating the system. In the limit of small distances $z \leq 10^{-3}\lambda_0$, the interaction of each emitter with the medium dominates regardless of the temperature and the two emitters behave independently. On the other hand, for larger distances $z \geq 10^{-1}\lambda_0$, one has a maximal superradiance independently of the temperature. In these situations, the emitters are hardly influenced by the material. In contrast, the tuning of the collective effects by the temperature is most effective in the intermediate range $z \simeq 5 \times 10^{-2}\lambda_0$. At these distances, the

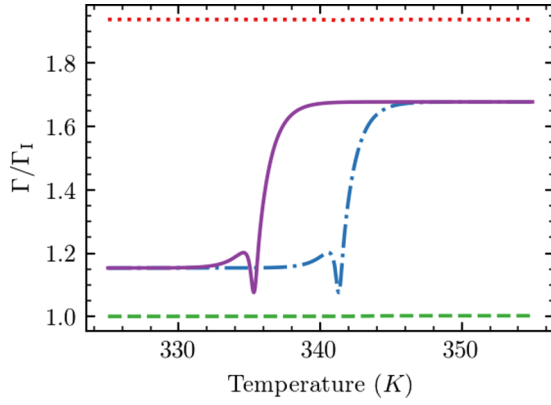


FIG. 5. Spontaneous emission rate in VO₂ normalized by the incoherent contribution for the symmetric state as a function of the temperature T at a separation $x = 0.1\lambda_0$ between emitters with transition wavelength $\lambda_0 = 450 \mu\text{m}$. The figure shows the emission rate for the cooling cycle at $z = 10^{-2}\lambda_0$ (solid purple line) and for the heating cycle at $z = 10^{-3}\lambda_0$ (green dashed line), $z = 10^{-2}\lambda_0$ (blue dashed-dotted line), and $z = 10^{-1}\lambda_0$ (red dotted line).

phase transition enhances quantum interferences between the emitters and the hysteresis is more pronounced, and thus more sensitive to the temperature.

V. CONCLUSION

In conclusion, we have shown that the presence of a critical medium significantly alters the decoherence experienced by a single emitter, as well as the collective quantum emission. These distinct physical phenomena, namely, the decoherence suffered by a single emitter in a coherent superposition of two wave packets and the collective decay process of two quantum emitters, have been addressed within a unified framework. Indeed, the decoherence rate and the collective emission rate are given in terms of the sum of an incoherent and a nonlocal contribution. The former is directly related to spontaneous emission process, whereas the latter encodes interference effects in the decoherence rate, or in the collective decay rate of two emitters.

We have found that the percolation phase transition in inhomogeneous media drastically suppresses the nonlocal contributions to the c.m. decoherence and to the collective emission by two emitters. One observes a slope discontinuity reminiscent of a “sudden death” of collective effects and nonlocal decoherence at the critical point. In the specific case of VO₂ undergoing a metal-insulator transition driven by temperature, the decoherence rate and collective emission exhibit a characteristic hysteresis leading to different behaviors in the cooling and heating cycles. This result suggests VO₂ as an alternative material platform to tune collective effects by means of a phase transition. Altogether, our results indicate that critical phenomena appear as a promising mechanism to control and tune light-matter interactions at the nanoscale.

ACKNOWLEDGMENTS

The authors are grateful to Paulo A. Maia-Neto, Daniela Szilard, Reinaldo F. de Melo e Souza, Marcelo França, and

Felipe Rosa for stimulating discussions. This work was supported by the Brazilian agencies CNPq, CAPES, and FAPERJ. F.A.P. also thanks The Royal Society-Newton Advanced Fellowship (Grant No. NA150208) for financial support. This work is part of INCT-IQ from CNPq.

APPENDIX: INFLUENCE OF THERMAL EFFECTS ON THE DECOHERENCE AND COLLECTIVE EMISSION RATES

In this Appendix, we extend the results discussed in the main text to account for a possible finite temperature of the electromagnetic (EM) field. Indeed, the assumption of an EM field in the vacuum state can appear as too restrictive, or even unrealistic, for emitters in the vicinity of a heated VO₂ material. In this Appendix, we thus consider instead the EM field at a finite temperature T , described through the following thermal density matrix [45],

$$\rho_{\text{EM}} = \prod_k \left[1 - \exp\left(-\frac{\hbar\omega_k}{k_B T}\right) \right] \exp\left(\frac{\hbar\omega_k a_k^\dagger a_k}{k_B T}\right), \quad (\text{A1})$$

where k_B is the Boltzmann constant. When evaluating the electric field Green’s function (7) and (8) with this thermal density matrix, the finite temperature merely introduces an additional factor $[n_{\omega_0}(T) + 1]$, where $n_{\omega_0}(T)$ is the average Bose-Einstein distributed photon number at the transition frequency ω_0 and for the temperature T . Thus, the thermal field raises a simple enhancement factor for the global decoherence rate $\Gamma^{\text{Dec}}(T) = [n_{\omega_0}(T) + 1]\Gamma^{\text{Dec}}(0)$, corresponding to the stimulated emission with thermal photons. Most importantly, the thermal field does not affect the decoherence profile as a function of the phase transition, nor the balance between the interference and the incoherent contributions to the total decoherence rate. The conclusions obtained for the decoherence rates with an EM field in the vacuum state thus still prevail at finite temperature.

We now investigate the influence of a finite EM field temperature on the collective emission. For this purpose, we use the field thermal density matrix (A1), assuming an EM field and the emitter DOF initially uncorrelated, and take the trace over the EM field DOF in the Born-Markov master equation [46],

$$\begin{aligned} \frac{\partial \rho_S}{\partial t}(t) = & \sum_{(m,n) \in \{1,2\}^2} [n_{\omega_0}(T) + 1] \frac{\Gamma_{mn}}{2} (2\sigma_m \rho_S \sigma_n^\dagger \\ & - \sigma_m^\dagger \sigma_n \rho_S - \rho_S \sigma_m^\dagger \sigma_n) \\ & + n_{\omega_0}(T) \frac{\Gamma_{mn}}{2} (2\sigma_m^\dagger \rho_S \sigma_n - \sigma_m \sigma_n^\dagger \rho_S - \rho_S \sigma_m \sigma_n^\dagger), \end{aligned} \quad (\text{A2})$$

with ρ_S the reduced density matrix corresponding to the emitters’ DOF, with the quantum operators σ_m acting upon the two-level emitter m as $\sigma_m |e_m\rangle = |g_m\rangle$ and $\sigma_m |g_m\rangle = 0$, and with the previously introduced dipole couplings Γ_{mn} (9). The population $\rho_{s,s}(t) = \langle s | \rho_S(t) | s \rangle$ in the symmetric state $|s\rangle = \frac{1}{\sqrt{2}}(|eg\rangle + |ge\rangle)$ follows the rate equation

$$\begin{aligned} \frac{\partial \rho_{s,s}}{\partial t} = & (\Gamma_I + \Gamma_C) [n_{\omega_0}(T) \rho_{gg,gg} + [n_{\omega_0}(T) + 1] \rho_{ee,ee} \\ & - [2n_{\omega_0}(T) + 1] \rho_{s,s}]. \end{aligned} \quad (\text{A3})$$

$\rho_{gg,gg}$ and $\rho_{ee,ee}$ denote the density matrix population for two emitters simultaneously in the ground state and in the excited state, respectively. From the equation above, we infer that the decay of the symmetric state is given by the rate $[2n_{\omega_0}(T) + 1](\Gamma_1 + \Gamma_C)$. The enhancement by a finite temperature factor $[2n_{\omega_0}(T) + 1]$ with respect to the vacuum EM field state corresponds to stimulated emission and is on the order of 20 for the temperatures and frequencies con-

sidered in the main text. Nevertheless, the ratio between the coherent contribution to the collective emission rate and the total emission rate remains unchanged by the finite field temperature. We conclude that taking into account thermal effects in the field itself on the collective emission does not qualitatively affect the suppression of the coherent contribution at the phase transition as well as the other findings presented in this paper.

-
- [1] R. H. Dicke, *Phys. Rev.* **93**, 99 (1954).
- [2] D. Martín-Cano, L. Martín-Moreno, F. J. García-Vidal, and E. Moreno, *Nano Lett.* **10**, 3129 (2010).
- [3] V. V. Temnov and U. Woggon, *Phys. Rev. Lett.* **95**, 243602 (2005).
- [4] J. Pan, S. Sandhu, Y. Huo, N. Stuhmann, M. L. Povinelli, J. S. Harris, M. M. Fejer, and S. Fan, *Phys. Rev. B* **81**, 041101(R) (2010).
- [5] J. J. Choquette, K.-P. Marzlin, and B. C. Sanders, *Phys. Rev. A* **82**, 023827 (2010).
- [6] R. Fleury and A. Alù, *Phys. Rev. B* **87**, 201101(R) (2013).
- [7] Y. Li and C. Argyropoulos, *Opt. Express* **24**, 26696 (2016).
- [8] P. A. Huidobro, A. Y. Nikitin, C. Gonzalez-Ballester, L. Martín-Moreno, and F. J. García-Vidal, *Phys. Rev. B* **85**, 155438 (2012).
- [9] P. Solano, P. Barberis-Blostein, F. K. Fatemi, L. A. Orozco, and S. L. Rolston, *Nat. Commun.* **8**, 1857 (2017).
- [10] B. Casabone, K. Friebe, B. Brandstatter, K. Schuppert, R. Blatt, and T. E. Northup, *Phys. Rev. Lett.* **114**, 023602 (2015).
- [11] X. Zeng, Z. Liao, M. Al-Amri, and M. S. Zubairy, *Europhys. Lett.* **115**, 14002 (2016).
- [12] D. Pavolini, A. Crubellier, P. Pillet, L. Cabaret, and S. Liberman, *Phys. Rev. Lett.* **54**, 1917 (1985).
- [13] T. Bienaimé, N. Piovella, and R. Kaiser, *Phys. Rev. Lett.* **108**, 123602 (2012).
- [14] M. Scheibner, T. Schmidt, L. Worschech, A. Forchel, G. Bacher, T. Passow, and D. Hommel, *Nat. Phys.* **3**, 106 (2007).
- [15] M. O. Scully, *Phys. Rev. Lett.* **115**, 243602 (2015).
- [16] W. Guerin, M. O. Araújo, and R. Kaiser, *Phys. Rev. Lett.* **116**, 083601 (2016).
- [17] A. Kalachev and S. Kroll, *Phys. Rev. A* **74**, 023814 (2006).
- [18] H. A. M. Leymann, A. Foerster, F. Jahnke, J. Wiersig, and C. Gies, *Phys. Rev. Appl.* **4**, 044018 (2015).
- [19] A. Kalachev, *Phys. Rev. A* **76**, 043812 (2007).
- [20] G. Gordon, G. Kurizki, and D. A. Lidar, *Phys. Rev. Lett.* **101**, 010403 (2008).
- [21] K. Sinha, B. P. Venkatesh, and P. Meystre, *Phys. Rev. Lett.* **121**, 183605 (2018).
- [22] E. M. Purcell, *Phys. Rev.* **69**, 37 (1946).
- [23] S. Fuchs and S. Y. Buhmann, *Europhys. Lett.* **124**, 34003 (2018).
- [24] N. de Sousa, J. J. Sáenz, A. García-Martín, L. S. Froufe-Pérez, and M. I. Marqués, *Phys. Rev. A* **89**, 063830 (2014).
- [25] N. de Sousa, J. J. Sáenz, F. Scheffold, A. García-Martín, and L. S. Froufe-Pérez, *Phys. Rev. A* **94**, 043832 (2016).
- [26] D. Szilard, W. J. M. Kort-Kamp, F. S. S. Rosa, F. A. Pinheiro, and C. Farina, *Phys. Rev. B* **94**, 134204 (2016).
- [27] V. Krachmalnicoff, E. Castanié, Y. De Wilde, and R. Carminati, *Phys. Rev. Lett.* **105**, 183901 (2010).
- [28] M. B. Silva Neto, D. Szilard, F. S. S. Rosa, C. Farina, and F. A. Pinheiro, *Phys. Rev. B* **96**, 235143 (2017).
- [29] J. I. Cirac and P. Zoller, *Phys. Rev. Lett.* **74**, 4091 (1995).
- [30] F. Impens, R. O. Behunin, C. C. Ttira, and P. A. Maia Neto, *Europhys. Lett.* **101**, 60006 (2013).
- [31] F. Impens, C. C. Ttira, and P. A. Maia Neto, *J. Phys. B* **46**, 245503 (2013).
- [32] F. Impens, C. C. Ttira, R. O. Behunin, and P. A. Maia Neto, *Phys. Rev. A* **89**, 022516 (2014).
- [33] R. de Melo e Souza, F. Impens, and P. A. Maia Neto, *Phys. Rev. A* **94**, 062114 (2016).
- [34] Note that when considering the decoherence of a single delocalized quantum emitter, we shall handle the position \mathbf{r} as a quantum operator.
- [35] L. Novotny and B. Hecht, *Principles of Nano Optics* (Cambridge University Press, Cambridge, UK, 2012).
- [36] D. A. G. Bruggeman, *Ann. Phys. (Berlin)* **416**, 636 (1935).
- [37] M. Sahimi, in *Applications of Percolation Theory* (Taylor and Francis, London, 1993), p. 59.
- [38] H. S. Choi, J. S. Ahn, J. H. Jung, T. W. Noh, and D. H. Kim, *Phys. Rev. B* **54**, 4621 (1996).
- [39] K. Sun, C. A. Riedel, A. Urbani, M. Simeoni, S. Mengali, M. Zalkovskij, B. Bilenberg, C. H. de Groot, and O. L. Muskens, *ACS Photon.* **5**, 2280 (2018).
- [40] P. Markov, R. E. Marvel, H. J. Conley, K. J. Miller, R. F. Haglund, Jr., and S. M. Weiss, *ACS Photon.* **2**, 1175 (2015).
- [41] M. M. Qazilbash, M. Brehm, G. O. Andreev, A. Frenzel, P. C. Ho, B. G. Chae, B. J. Kim, S. J. Yun, H. T. Kim, A. V. Balatsky, O. G. Shpyrko, M. B. Maple, F. Keilmann, and D. N. Basov, *Phys. Rev. B* **79**, 075107 (2009).
- [42] D. B. Hough and L. R. White, *Adv. Colloid Interface Sci.* **14**, 3 (1980).
- [43] M. A. Ordal, R. J. Bell, R. W. Alexander, Jr., L. L. Long, and M. R. Querry, *Appl. Opt.* **24**, 4493 (1985).
- [44] At the separation $x = 0.7\lambda_0$, the free-space c.m. decoherence rate is enhanced by a positive interference term involving the two emitting wave packets [33]. In the metallic phase, for a perfect conductor, the scattering contribution to the c.m. decoherence rate can be obtained by using the image dipoles (with respect to the material interface) associated with the emitting wave packets. Interferences similar to the free-space contribution are then obtained. This is no longer valid for the material in the insulator phase.
- [45] L. Mandel and E. Wolf, *Optical Coherence and Quantum Optics* (Cambridge University Press, Cambridge, UK, 1995).
- [46] H.-P. Breuer and F. Petruccione, *Theory of Open Quantum Systems* (Oxford University Press, New York, 2002).